LATTICE SHRINKAGE WITH INCREASING RESTING TENSION IN STRETCHED, SINGLE SKINNED FIBERS OF FROG MUSCLE

HIDEO HIGUCHI AND YOSHIKI UMAZUME
Department of Physiology, The Jikei University School of Medicine, Tokyo 105, Japan

ABSTRACT   The 1,0 lattice spacing $d_{1,0}$ in chemically and mechanically skinned single fibers of frog muscle was measured at various sarcomere lengths, L, in the range from $L = 2.1$ to 6.0 μm by an x-ray diffraction method. In chemically skinned fibers, $d_{1,0}$ decreased with a similar slope to that of mechanically skinned fibers up to $L \simeq 3$ μm, but beyond this point $d_{1,0}$ steeply decreased with further stretching. This steep decrease in $d_{1,0}$ could be ascribed mainly to an increase in the compressing force associated with the longitudinal extension of a remnant of the sarcolemma. In mechanically skinned fibers, the gradual decrease in $d_{1,0}$ continued beyond filament overlap ($L \geq 3.5$ μm) and was highly proportional to a resting tension. This decrease in $d_{1,0}$ at $L \geq 3.5$ μm could be ascribed to an increase in the force exerted by lateral elastic components, which is proportional to the longitudinal resting tension. A conceptual model is proposed of a network structure of elastic components in a sarcomere.

INTRODUCTION

The sarcomere volume in living striated muscle remains constant (isovolumic) over a wide range of the length of muscle so that the filaments move nearer together when a muscle is stretched (Huxley, 1953). Matsubara and Elliott (1972) first demonstrated that a skinned fiber of frog no longer behaved isovolumically, and the lattice spacing $d_{1,0}$ decreased linearly with the sarcomere length L when the fiber was stretched from $L = 2.1$ to 3.5 μm. This particular behavior in the skinned fiber could be explained in terms of the variation of negative charge within the A-band with interdigitation of thin filaments (Elliott, 1973).

Higuchi and Umazume (1985) measured the resting tension of extremely stretched skinned fibers ($3.5 \leq L \leq 6.0$ μm) in which the A-band was partially dissociated at high ionic strengths. Based on the relation between the residual length of A-band and the resting tension, the authors predicted the presence of parallel elastic components that might contribute to the force balance in the filament lattice (see the *right* half of Fig. 4 *b*, given later).

Here we studied the relation between $d_{1,0}$ and L over the range from 2.1 to 6.0 μm in relaxed single skinned fibers. For mechanically skinned fibers, we found that the gradual decrease in $d_{1,0}$ continued beyond the filament overlap and was highly proportional to a longitudinal resting tension. The decrease in $d_{1,0}$ associated with the stretch is explained in terms of the lateral elastic force that is proportional to the longitudinal resting tension. To account for the present observation, the previous model (Higuchi and Umazume, 1985) is revised such that the parallel elastic components bind to the lateral elastic components between thick filaments.

METHODS

Specimens

Fibers from semitendinosus muscle of frog (*Rana catesbeiana*) were used. A single fiber segment was mechanically skinned (Natori, 1954) in a relaxing solution (90 mM KCl, 5.2 mM $MgCl_2$, 4.3 mM Na_2ATP, 4.0 mM EGTA, 10 mM PIPES, pH 7.0 at 20°C). To destroy the sarcoplasmic reticulum, the mechanically skinned fiber was incubated for 15 min in the relaxing solution containing 0.5% Brij-58.

In part of the experiments, chemically skinned fibers were also prepared by referring to the procedure described in Magid and Reedy (1980): a single fiber segment was incubated for 15 min in the relaxing solution containing 0.5% Triton X-100. After this treatment, the chemically skinned fiber in an activating solution containing 10^{-5} M Ca^{2+} developed an active force of $\sim 2 \times 10^5$ N/m^2 at $L = 2.1$ μm, suggesting that chemical skinning was complete. All the experimental procedures were performed at 20°C.

X-ray Diffraction

For measuring $d_{1,0}$, an x-ray diffraction method was employed. The apparatus was the same as that in Umazume et al. (1986). A segment of a skinned fiber was held vertically in a specimen chamber by connecting both ends with thin threads to stainless steel shafts (0.3 mm in diam and 4 mm in length) with a separation of 8 mm. After mounting a fiber, its length was adjusted to a given L monitored by an optical diffraction method. The chamber with mylar windows (3 × 8 mm²) had a capacity of 0.09 ml and was connected to a peristaltic pump (model SJ-1221; ATTO Co., Tokyo, Japan) to perfuse a given solution at a rate of 0.4 ml/min. The path length in the chamber was 0.5 mm. The equatorial x-ray diffraction pattern was recorded by a double-mirror Franks camera (Franks, 1955; Elliott and Worthington, 1963). The x-ray source was a rotating-anode generator (model RU-200; Rigaku Electric Co., Tokyo, Japan) with a fine focus (1 × 0.1 mm²) on a copper target (viewed at an angle of 3°). This was operated at 40 kV with a tube current of 30 mA. The specimen-film distance was 227 mm, and most of the beam path was evacuated. The exposure time used to record the equatorial diffraction pattern on x-ray film (DEF-5; Eastman Kodak Co., Rochester, NY) was

30–60 min. The 1,0 reflections from the hexagonal myofilament lattice were clearly observed, but 1,1 reflections were much weaker than those of intact fibers. If diffraction patterns were recorded repeatedly in a given fiber, the intensities of the 1,0 reflections gradually decreased. Therefore, a single diffraction pattern was recorded for each fiber. The positions of the 1,0 reflections were measured with a comparator (model V-12; Nikon Inc., Tokyo, Japan) to obtain the $d_{1,0}$ value.

Measurements of Resting Tension

Independently of x-ray diffraction studies, the resting tension of mechanically and chemically skinned fibers in the relaxing solution was measured at various L's. The method for measuring the cross-sectional area A^* (at $L = 2.5 \mu m$) and the tension T_{obs} of a fiber was the same as that in Higuchi and Umazume (1985). The resting tension was scaled as $T = T_{obs}/A^*$ in units of N/m². Let A_c^* be the cross-sectional area occupied by one thick filament at $L = 2.5 \mu m$. Since myofilaments occupy only ~80% of the cross-sectional area (Schoenberg, 1980), $M = 0.8 A^*/A_c^*$ is the number of thick filaments in a fiber. Therefore, the tension per filament is given by $t = T_{obs}/M = T \cdot A_c^*/0.8$ in units of N. (Note that $A_c^* = 2d_{1,0}^{*2}/\sqrt{3}$, where $d_{1,0}^*$ is the 1,0 lattice spacing at $L = 2.5 \mu m$; see Fib. 4 a given later). This scale of tension was also used if necessary.

When the fiber was stretched suddenly to $L \geq 3.5 \mu m$, an instantaneous increase in the tension was followed by an exponentially decreasing phase with a relaxation time of ~10 min. At ~45 min after stretching, the tension reached almost a steady level, and this steady value of the tension was defined to be a resting tension, T. The resting tension was ~20–30% of instantaneously increased tension. If a fiber previously stretched to $L \geq 3.5 \mu m$ was released to a given L, the tension reached a much smaller value than the resting tension at the same L without previous stretch. Because of this, the resting tension was measured once for each fiber at $L \geq 3.5 \mu m$.

RESULTS

Relation between Lattice Spacing and Sarcomere Length

About 20 min after setting the fiber in the specimen chamber, the x-ray exposure was started and continued for 30 min at $L \leq 3.0 \mu m$ and for 40–60 min at $3.5 \leq L \leq 6.0 \mu m$. Both mechanically and chemically skinned fibers gave sharp 1,0 equatorial reflections at all L's. Fig. 1 shows the

relations between $d_{1,0}$ and L. The $d_{1,0}$ at $L = 2.1 \mu m$ was 41.9 ± 0.4 nm (mean ± SD, $n = 6$) and 40.8 ± 0.3 nm ($n = 3$) in mechanically and chemically skinned fibers, respectively. The $d_{1,0}$ of mechanically skinned fibers decreased sigmoidally with increasing L, and $d_{1,0}$ was 35.1 ± 0.3 nm ($n = 6$) at $L = 6.0 \mu m$. In chemically skinned fibers, $d_{1,0}$ decreased with a similar slope to that of mechanically skinned fibers up to $L = 3.0 \mu m$, but beyond this point $d_{1,0}$ started to drop steeply with further stretching, and $d_{1,0}$ was 27.7 ± 0.6 nm ($n = 3$) at $L = 4.0 \mu m$. The chemically skinned fiber broke in two at $L \simeq 4.5 \mu m$.

Relation Between Resting Tension and Sarcomere Length

The resting tension was measured at each L corresponding to the data in Fig. 1. The resting tension of mechanically skinned fibers increased sigmoidally with increasing L and reached $(3.6 \pm 0.5) \times 10^4$ N/m² ($n = 3$) at $L = 6.0 \mu m$ (Fig. 2). In chemically skinned fibers, the resting tension increased in a similar fashion to that of mechanically skinned fibers up to $L = 3 \mu m$, but beyond this point it started to rise steeply with further stretching and was $(8.6 \pm 0.5) \times 10^4$ N/m² ($n = 3$) at $L = 4.0 \mu m$.

Relation between Lattice Spacing and Resting Tension

The relation between $d_{1,0}$ and the resting tension of mechanically skinned fibers was obtained from Figs. 1 and 2, and is shown in Fig. 3. These two quantities were highly correlated. The lattice spacing $d_{1,0}$ (in nanometers), from the least-squares linear regression line plotted over the range from $d_{1,0} = 41.9$ to 35.1 nm (corresponding to $L = 2.1$–$6.0 \mu m$), was

$$d_{1,0} = aT + 41.9 \text{ nm} \quad (r = 0.999), \quad (1a)$$

where $a = -1.87 \times 10^{-13}$ m³/N and T is the resting

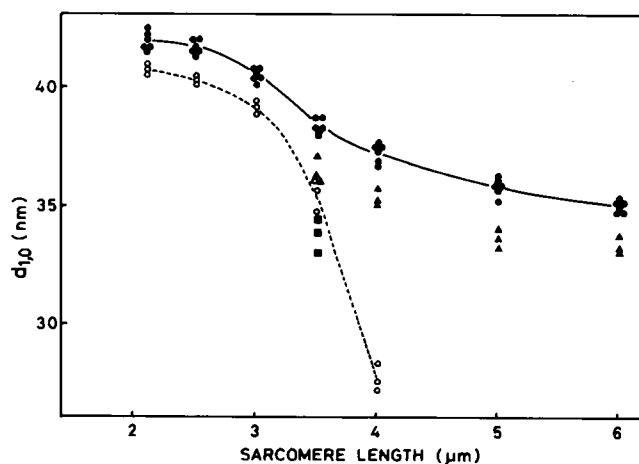

FIGURE 1 Relations between $d_{1,0}$ and L. (O) Chemically skinned fibers in 0% PVP, (●) mechanically skinned fibers in 0% PVP, (▲) in 1% PVP and (■) 2% PVP. Lines were drawn by inspection.
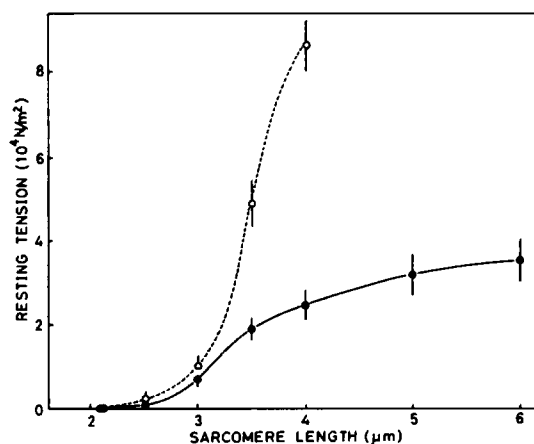

FIGURE 2 Relations between the resting tension (T) and L. (O) Chemically skinned fibers and (●) mechanically skinned fibers. Data of mechanically skinned fibers include those in Higuchi and Umazume (1985). Symbols and bars indicate means and SD, respectively.

386

tension in 10^4 N/m^2 (the solid line in Fig. 3), or from $t = T$ $\cdot A_c^*/0.8$ (see Methods) we have

$$d_{1,0} = bt + 41.9 \text{ nm}, \tag{1b}$$

where $b = -7.45 \times 10$ m/N, and t is in 10^{-10} N.

Radial Compression

A set of experiments was carried out to estimate the magnitude of the force to decrease $d_{1,0}$ when the mechanically skinned fibers were stretched. To give an osmotic compressing force to a fiber, PVP (polyvinylpyrrolidone, PVP K-30, $M_n = 40,000$, Tokyo Kasei) was added to the relaxing solution (Godt and Maughan, 1977). The pH value of the solution decreased on addition of PVP; pH at 2% PVP, for example, was ~0.2 unit lower than that at 0% PVP. Therefore, pH was readjusted with KOH after adding PVP. At $L = 3.5$ μm, $d_{1,0}$'s were 38.3 ± 0.3 nm ($n = 6$), 36.5 ± 0.5 nm ($n = 3$), and 33.6 ± 0.8 nm ($n = 3$) in 0, 1, and 2% PVP solutions, respectively (Fig. 1). The pressure due to added PVP was calculated by using the empirical equation given by Vink (1971). The $d_{1,0}$ decreased in proportion to the osmotic pressure in the range studied. The least-squares linear regression line at $L = 3.5$ μm was

$$d_{1,0} = cP + 38.3 \text{ nm} \quad (r = 0.974), \tag{2}$$

where $c = -1.99 \times 10^{-12}$ m^3/N and P is the osmotic pressure (or the compressing force) in 10^3 N/m^2 and $d_{1,0}$ in nm. In 1% PVP, $d_{1,0}$'s were 35.3 ± 0.4 ($n = 3$), 33.6 ± 0.4 ($n = 3$) and 33.4 ± 0.4 ($n = 3$) nm at $L = 4.0$, 5.0, and 6.0 μm, respectively (Fig. 1). In the 95% confidence limit, slopes of $d_{1,0}$ against P in 0 and 1% PVP were (-2.05 ± 0.66), (-2.34 ± 0.69), and (-1.75 ± 0.55) in units of 10^{-12} m^3/N at $L = 4.0$, 5.0, and 6.0 μm, respectively; these slopes were not significantly different from (-1.99 ± 0.39) $\times 10^{-12}$ m^3/N in Eq. 2.
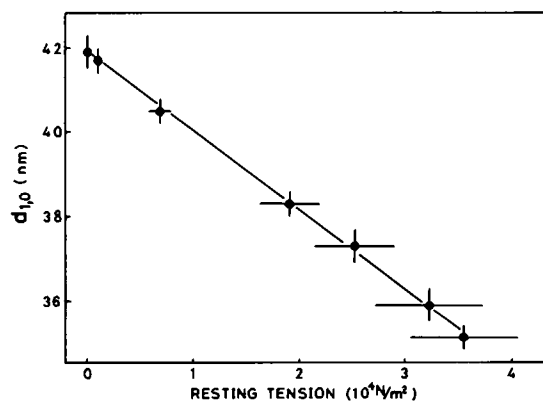

FIGURE 3 Relation between the resting tension (T) and $d_{1,0}$ of mechanically skinned fibers. Data were taken from Figs. 1 and 2. The solid line shows the regression line in Eq. 1a.

DISCUSSION

Here it was shown that the resting tension of chemically skinned fibers was much larger than that of mechanically skinned fibers at $L \gtrsim 3.0$ μm. This result agrees with those for sartorius muscle of *Bufo bufo japonicus* (Natori, 1954), semitendinosus muscle of *Rana pipiens* (Podolsky, 1964) and sartorius muscle of *Rana catesbeiana* (Umazume, 1974). All these results suggest that the sarcolemma mostly contributes to the resting tension at $L \gtrsim 3$ μm. In addition, $d_{1,0}$ of chemically skinned fibers decreased steeply at $L \gtrsim 3.0$ μm (Fig. 2). This result confirmed the studies by Shapiro et al. (1979) and Magid and Reedy (1980). Shapiro et al. (1979), for example, reported that the decrease in $d_{1,0}$ with L was very small until a definite break point was reached (at ~3 μm), which appeared to coincide with L where the resting tension became measurable. Then, it is likely that the steep decrease in $d_{1,0}$ at $L \gtrsim 3$ μm in the chemically skinned fibers is attributed mainly to the lateral compressing force associated with the longitudinal extension of remnants of the sarcolemma and collagen sheath surrounding a fiber.

In the mechanically skinned fibers, $d_{1,0}$, also decreased with increasing L (Fig. 1). In the range 2.1 ≤ L ≤ 3.5 μm, our observation confirmed that the result by Matsubara and Elliott (1972). The decrease in $d_{1,0}$ with stretching in this range was explained in terms of the negative charge within the A-band with interdigitation of thin filaments (Elliott, 1973). Even in fibers stretched to $L \geq 3.5$ μm, we could also observe clear equatorial diffraction patterns and obtain a definite relation between $d_{1,0}$ and L. When L was increased from 3.5 to 6.0 μm, $d_{1,0}$ decreased significantly from 38.3 to 35.1 nm. The observed change in $d_{1,0}$ at $L \geq 3.5$ μm cannot be explained by the Elliott model (1973), because thin filaments no longer exist in the A-band.

What are the underlying reasons for the decrease in $d_{1,0}$ of the mechanically skinned fibers with stretching? Toyoda and Maruyama (1978) showed that the elastic components form three dimensional networks in a sarcomere. Wang and Ramirez-Mitchell (1983) reported that the elastic filaments surround each myofibril in a muscle fiber. Magid et al. (1984) observed many structures that laterally connect neighboring thick filaments. These elements would behave as "lateral elastic components" (LECs) and "parallel elastic components" (PECs) in mechanically skinned fibers. It is possible that PECs bind to LECs (Higuchi and Umazume, 1985). Therefore, when the fiber is stretched, LECs would exert a force (F), which would tend to pull thick filaments nearer together.

The relationship between the compressing force and the resting tension can be analyzed as follows. The slopes $\Delta d_{1,0}/\Delta P$ at $L \geq 3.5$ μm were not significantly different from each other, where ΔP is the increment in P required to induce a given amount of the decrement $\Delta d_{1,0}$ in $d_{1,0}$. The $d_{1,0}$'s were also obtained at $L = 2.5$ μm (Umazume et al., 1986): $d_{1,0}$'s were 41.3, 40.0, and 36.9 nm in 0%, 1%, and 2% PVP, respectively, and $\Delta d_{1,0}/\Delta P$ was calculated to be

1.96 $\times$ 10^{-12} m^3/N, which is very close to those at $L \geq 3.5$ μm. Therefore, it is likely that $\Delta d_{1,0}/\Delta P$ has the same value at any L in the range from 2.5 to 6.0 μm and at any $d_{1,0}$ in the range from 41.3 to 35.1 nm; i.e., $\Delta d_{1,0} \propto \Delta P$. Fig. 3 indicates $\Delta d_{1,0} \propto \Delta T$, where ΔT is the increment in T required to induce $\Delta d_{1,0}$. Thus, $\Delta P \propto \Delta T$; i.e., the increment ΔF in F produced by stretching the fiber to induce a given $\Delta d_{1,0}$ is therefore equivalent to ΔP required to induce the same $\Delta d_{1,0}$.

Forces per a half thick filament to induce $\Delta d_{1,0} = 1$ nm can be estimated as follows, where the compressing force Δp is produced by the osmotic pressure, the lateral force Δf ($=\Delta p$) is produced by LECs, and the longitudinal force Δt is produced by PECs. Following the method of Schoenberg (1980), we consider an elementary volume, hexagonal in cross-section, with a length of $L_A/2$ (L_A being the length of the thick filament) as shown in cross-section in Fig. 4 *a*. The surface area around the circumference of this elementary column is equal to $A_s = 2d_{1,0} \cdot L_A$, and the cross-sectional area $A_c = 2d_{1,0}^2/\sqrt{3}$. Taking $d_{1,0} = 38$ nm (corresponding to $L = 3.5$ μm) and $L_A = 1.5$ μm, we have Δp ($=\Delta f$) $= \Delta P \cdot A_s = 6.0 \times 10^{-11}$ N. (The compressing force P to induce $\Delta d_{1,0} = 1$ nm is given by Eq. 2; $\Delta P = 5.0 \times 10^2$ N/m^2). Thus, from Eq. 1b, $\Delta t = 1.3 \times 10^{-11}$ N. In this case, $\tan\theta = \Delta p/\Delta t \simeq 4.6$ or $\theta \simeq 78°$, where θ is the angle between the force vectors of LEC and PEC (see the *left* half of Fig. 4 *b*).

The value of the radial stiffness in KCl-ghost fibers (skinned fibers from which thick filaments were extracted) was about one half of that in skinned fibers (unpublished observation). Thus the I-bands do contribute to the lateral (repulsive) force, but for our order-of-magnitude estimations of the relevant forces this contribution was neglected.

In the above discussion, the osmotic pressure was calculated by assuming that no PVP entered the lattice. However, Matsubara et al. (1984) noted that PVP does enter the lattice. By assuming that the distribution of molecular weight of PVP inside the lattice is the same as that in the external medium, they estimated the osmotic pressure difference between the inside and outside the lattice. If we apply their method to the present condition at $L = 3.5$ μm, $\Delta d_{1,0}/\Delta P$ is calculated to be 7.94 $\times$ 10^{-12} m^3/N and hence Δp to be 9 $\times$ 10^{-12} N. In this case, $\tan \theta \simeq 0.7$ or $\theta \simeq 35°$.

If we assume no entry of PVP, Fig. 3 suggests no appreciable contribution of the electrical repulsive force at $L \leq 3.5$ μm. But if we also apply the method of Matsubara et al. (1984) to evaluate $d_{1,0}$ vs. P relation at $L = 2.5$ μm, $\Delta d_{1,0}/\Delta P$ is calculated to be 4.83 $\times$ 10^{-12} m^3/N, which is significantly smaller than that at $L = 3.5$ μm. That is, the repulsive force opposing P is estimated to be greater at $L = 2.5$ μm than that at $L = 3.5$ μm. If this is the case, one of the possible origins of the greater repulsive force may be the negative charge within the A-band with interdigitation of thin filaments (Elliott, 1973). In this case, stretching the fiber to reduce the overlap between thick and thin filaments would lead to a smaller repulsive force and a larger F. Therefore, the net amount of the force to induce a given $\Delta d_{1,0}$ with stretching would be $\Delta F + \Delta R$, where ΔR is the decrement in the repulsive force. Then, we have a relationship $\Delta F + \Delta R = \Delta P \propto \Delta T$ at $L \leq 3.5$ μm.

The above consideration leads to a conceptual model, as shown in Fig. 4, of a network structure of elastic components in a sarcomere. This model is a revised version of our previous one (Fig. 9 in Higuchi and Umazume, 1985; the *right* half of Fig. 4 *b*), and again shows only an equivalent network of elastic components. At $L \leq 4$ μm, the PECs connecting Z-lines (not shown in Fig. 4; see "zig-zag lines" in Higuchi and Umazume, 1985) are slack and do not contribute to the resting tension. The following point must be mentioned. At $L \geq 5$ μm, ~35% of the resting tension may be ascribed to the PECs connecting Z-lines (Higuchi and Umazume, 1985). Since the width of KCl- and KI-ghost fibers (fibers from which thick filaments and
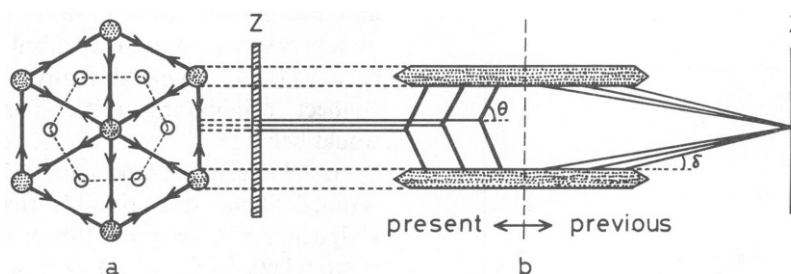

FIGURE 4   A conceptual model of a network structure of elastic components in a sarcomere. This model is concerned with only the present observation and the previous one (Higuchi and Umazume, 1985). (*a*) Cross-section of the thick filament lattice. Large circles denote thick filaments, and small circles denote the positions of thin filaments at $L \leq 3.5$ μm. Dashed lines indicate the circumference of the elementary volume (Schoenberg, 1980), which includes only one thick filament and can cover all the myospace by its translation. Solid lines show the lateral elastic components (LECs) connecting thick filaments. The components (perpendicular to thick filaments) of the forces exerted by LECs are indicated by arrows, which are also perpendicular to the surfaces of the elementary volume. Each parallel elastic component (PEC) runs from the center of a LEC to a nearby Z-line (see *b*). (*b*) *Left* half; a conceptual drawing of distribution of LECs (thick lines) and PECs (thin lines) in the 1,0 plane. The thin filaments exist off the plane of the sheet, so that both LECs and PECs may not interfere the cross-bridge/actin interaction. The elastic components directly connecting Z-lines (zig-zag lines in Higuchi and Umazume, 1985) are not shown here. *Right* half; the previous model proposed in Higuchi and Umazume (1985).

both thick and thin filaments were extracted, respectively) decreases with stretching, these PECs may be partly responsible for reducing $d_{1,0}$ at longer L's. If we adopt our previous model, $\tan \delta \simeq d_{1,0}/L$ is estimated to be ~0.01 or $\delta \simeq 0.6°$, where δ is an angle between longitudinal and lateral force vectors (see the *right* half of Fig. 4 *b*). Here, however, our estimation of the angle θ ($35° \leq \theta \leq 78°$) is about a hundredfold greater than the angle δ. Therefore, we propose a Y-shaped structure composed of a LEC and a PEC, instead of the previously proposed V-shaped structure (Fig. 4 *b*). In particular, because of the LECs that connect neighboring thick filaments, a longitudinal resting tension T can produce a large lateral force F.

REFERENCES

Elliott, G. F. 1973. Donnan and osmotic effects in muscle fibers without membranes. *J. Mechanochem. Cell Motil.* 2:83–89.

Elliott, G. F., and C. R. Worthington. 1963. A small-angle optically focusing x-ray diffraction camera in biological research. Part I. *J. Ultrastruct. Res.* 9:166–170.

Franks, A. 1955. An optically focusing x-ray diffraction camera. *Proc. R. Soc. Lond. B. Biol. Sci.* 68:1054–1064.

Godt, R. E., and D. W. Maughan. 1977. Swelling of skinned muscle fibers of the frog. Experimental observation. *Biophys. J.* 19:103–116.

Higuchi, H., and Y. Umazume. 1985. Localization of the parallel elastic components in frog skinned muscle fibers studied by the dissociation of A- and I-bands. *Biophys. J.* 48:137–147.

Huxley, H. E. 1953. X-ray analysis and the problem of muscle. *Proc. R. Soc. Lond. B. Biol. Sci.* 141:59–62.

Magid, A., and M. K. Reedy. 1980. X-ray diffraction observations of chemically skinned frog skeletal muscle processed by an improved method. *Biophys. J.* 30:27–40.

Magid, A., H. P. Ting-Beall, M. Carvell, T. Kontis, and C. Lucaveche. 1984. Connecting filaments, core filaments, and side-struts: a proposal to add three new load-bearing structures to the sliding filament model. *In* Contractile Mechanisms in Muscle. G. H. Pollack and H. Sugi, editors. Plenum Publishing Corp., New York. 307–328.

Matsubara, I., and G. F. Elliott. 1972. X-ray diffraction studies on skinned single fibers of frog skeletal muscle. *J. Mol. Biol.* 72:657–669.

Matsubara, I., Y. E. Goldman, and R. M. Simmons. 1984. Changes in the lateral filament spacing of skinned fibers when cross-bridges attach. *J. Mol. Biol.* 173:15–33.

Natori, R. 1954. The role of myofibrils, sarcoplasm and sarcolemma. *Jikeikai Med. J.* 1:18–28.

Podolsky, R. J. 1964. The maximum sarcomere length for contraction of isolated myofibrils. *J. Physiol.* (*Lond.*). 170:110–123.

Schoenberg, M. 1980. Geometrical factors influencing muscle force development. II. Radial forces. *Biophys. J.* 30:69–78.

Shapiro, P. J., K. Tawada, and R. J. Podolsky. 1979. X-ray diffraction of skinned fibers. *Biophys. J.* 25(2, Pt. 2):18*a*. (Abstr.)

Toyoda, N., and K. Maruyama. 1978. Fine structure of connectin nets in cardiac myofibrils. *J. Biochem.* 84:239–241.

Umazume, Y. 1974. The elastic property of the frog skinned muscle fibers. *Jikeikai Med. J.* 21:11–24.

Umazume, Y., S. Onodera, and H. Higuchi. 1986. Width and lattice spacing in radially compressed frog skinned muscle fibers at various pH values, magnesium ion concentrations and ionic strengths. *J. Muscle Res. Cell Motil.* In press.

Vink, H. 1971. Precision measurements of osmotic pressure in concentrated polymer solutions. *Eur. Polym. J.* 7:1411–1419.

Wang, K., and R. Ramirez-Mitchell. 1983. A network of transverse and longitudinal intermediate filaments is associated with sarcomeres of adult vertebrate skeletal muscle. *J. Cell Biol.* 96:563–570.